ACS APPLIED NANO MATERIALS

www.acsanm.org Article

Tuning Fermi Energy of Graphene Using Platinum Nanoparticles and Ultraviolet Irradiation to Increase Charge Transfer for Surface-Enhanced Raman Spectroscopy

Samar Ali Ghopry,* Bo Liu, Andrew Shultz, and Judy Z. Wu*

Cite This: *ACS Appl. Nano Mater.* 2023, 6, 21626−21633 Read Online

ACCESS | Metrics & More | Article Recommendations

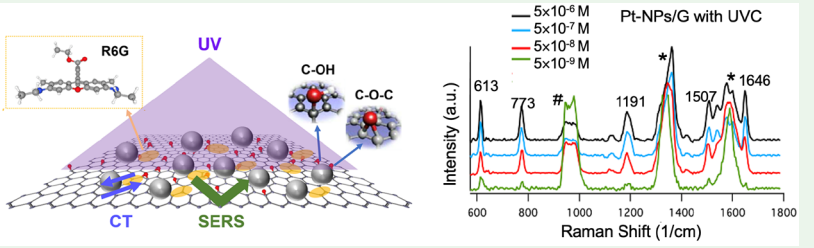

ABSTRACT: Surface-enhanced Raman spectroscopy (SERS) is an important analytical tool with ultrahigh sensitivity that depends on electromagnetic mechanism (EM) and chemical mechanism (CM). The CM relies on efficient charge transfer between the probe molecules and SERS substrates, which means engineering the molecule attachment and the energy level alignment at the molecule/substrate interface is critical to optimal CM enhancement. Herein, we report enhanced CM of Rhodamine 6G (R6G) on graphene SERS substrates using combined C-band ultraviolet (UVC) irradiation and Pt nanoparticle (Pt-NPs) decoration using atomic layer deposition (ALD). An enhancement of 270% was obtained in the former, which is ascribed to the graphene surface activation and p-doping on graphene for improved R6G molecule attachment and charge transfer by its surface change from hydrophobic to hydrophilic and the down-shift of the Fermi energy (p-doping) after UVC exposure. The Pt-NPs decoration adds an additional enhancement of 250% by further p-doping graphene, which shifts the graphene's Fermi energy to promote charge (hole) transfer at the R6G/graphene interface. Remarkably, the combination of the UVC irradiation and Pt-NPs decoration has led to enhanced R6G SERS sensitivity of 5×10^{-9} M, which represents a two-orders of magnitude enhancement over that on the pristine graphene and illustrates the importance of graphene engineering for optimal probe molecule attachment and the energy level alignment at the molecule/graphene interface toward achieving high-performance SERS biosensing.

KEYWORDS: *Surface-enhanced Raman spectroscopy, charge transfer, Pt nanoparticle, C-band ultraviolet, Rhodamine 6G*

1. INTRODUCTION

Surface-enhanced Raman spectroscopy (SERS) is an important method for detecting molecules with ultrahigh sensitivity.[1−4] By improving the Raman signatures of molecules, SERS can enable high sensitivity biosensing with detection limit of a single molecule.[1,5,6] SERS involves two mechanisms: electromagnetic enhancement (EM) and chemical enhancement (CM). The EM regards the local electromagnetic field enhancement that is typically attributed to the localized surface plasmonic resonance (LSPR).[7,8] The EM enhancement factor can reach over 10^8 to enable ultrasensitive SERS detection down to the single-molecule level.[9−11] Among other metal nanostructures, metal nanoparticles (NPs) such as Ag and Au NPs have been widely adopted for high EM effect in SERS because of their unique LSPR that depends on the size and shape of the NPs.[12,13] On the other hand, porous metallic nanostructures have also been explored for EM enhancement.[14−17] More recently, high EM enhancement factors have also been reported on nonmetallic nanostructures such as transition-metal dichalcogenides (TMDC) nanodiscs and nanodonuts.[18−20]

The CM is induced by charge transfer between the SERS substrate and probe molecules with an enhancement factor typically on the order of 10^1 to 10^3 as reported previously.[21−23] The CM effect is dictated by the analyte/substrate interface electronic structures and can be optimized by selecting a substrate with favorable band alignment with the highest-occupied molecular orbital (HOMO) and/or the lowest-unoccupied molecular orbital (LUMO) at the interface where

Received: August 4, 2023
Revised: October 30, 2023
Accepted: October 31, 2023
Published: November 20, 2023

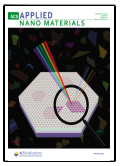

the analyte (or probe molecules) bonds to the substrate. Therefore, tuning of the SERS substrate's electronic structure is important for obtaining an enhanced CM effect.[24] This has prompted an intensive research in exploring graphene-based SERS substrates considering the unique two-dimensional (2D) atomically flat surface with delocalized π bonds, chemical inertness, biological compatibility, superior electronic and photonic properties, and the intrinsic Fermi energy at ~4.5 eV that is compatible, as well as tunable, for CM enhancement with a large number of probe molecules.[21−23,25,26] This means that graphene is an excellent candidate for SERS by providing a large surface for probe molecules to attach and Fermi level tunability for high CM enhancement.[6,22] Interestingly, the CM enhancement factor has been reported on graphene substrate.[27] For example, Ling et al. reported SERS CM enhancement factors of 2−17 on graphene substrate testing multiple probe molecules including R6G.[22] Different groups reported CM enhancement factors of 63, 13, and 16 on graphene, h-BN, and MoS_2, respectively, taking the 1531 cm^{-1} mode of CuPc molecules.[28]

In this work, we explore further enhancement of the SERS CM effect of graphene by combining two new approaches on tuning of the Fermi energy of the graphene using Rhodamine 6G (R6G) as the probe molecules. One approach is to activate the graphene surface using C-band ultraviolet (UVC) irradiation on graphene to down-shift the Fermi energy of graphene (p-doping) to enhance charge transfer across the R6G/graphene interface. The other is to decorate Pt nanoparticles (Pt-NPs) on graphene using conformal atomic layer deposition (ALD) to further down-shift the Fermi energy of graphene for improved energy level alignment at the R6G/graphene interface for improved charge (hole) transfer. It should be noted that UVC photons have fairly high energies of 4.9 eV (wavelength of 254 nm) and 6.7 eV (wavelength of 185 nm), which can effectively break the carbon−carbon bond on graphene. The UVC generated ozone may promote formation of C−O group, resulting in p-doping to graphene.[6,29] In addition, UVC irradiation may bring an additional benefit of improved R6G probe molecule attachment to graphene through activation of the carbon−carbon bonds. On the other hand, Pt has its work function in the range of 5.1−5.9 eV. The decorated Pt-NPs on graphene may generate p-doping to shift the Fermi energy of the graphene from intrinsic value of ~4.5 eV to higher values, in a similar way to the case of Au-NPs decorated graphene[27] for favorable alignment with R6G's HOMO experimentally measured onset and peak is 4.94−5.15 eV[30] for enhanced hole transfer at R6G/graphene interface. While Au-NPs decoration has been shown to enhance both EM and CM of R6G SERS signature, Pt has been found to have a negligible EM effect which means the Pt's SERS enhancement is primarily via CM effect.[31−33] For example, Cai et al. studied Raman spectra of Pyridine on Pt substrate and observed a SERS enhancement factor of about 2 orders of magnitude.[32] This enhancement is considered from CM contribution,[31] as the Raman intensity-potential profiles study shows the intensity peak position shifts when the excitation line changes from 632.8 to 514.5 nm which reveals the Fermi level shift at the electrode surface.[33] Since Pt-NPs could be conformally coated on samples via ALD,[34,35] this work explores superposition of the Fermi energy shifts by UVC irradiation and Pt-NPs decoration for improved CM effect of graphene. Remarkably, significantly enhanced R6G sensitivity has been obtained on these UVC-irradiated Pt-NP decorated graphene (Pt-NPs/graphene) substrates, illustrating the importance of the SERS CM effect for high-sensitivity SERS.

Figure 1 exhibits the UVC-treated Pt-NPs/graphene SERS substrate. The Pt-NPs are shown as gray spheres decorated on graphene using ALD. The deposited R6G molecules (purple) are expected to be on the SERS substrate with a weak interface to graphene via van der Waals (vdW) interaction. It should be noted that any unintended species, such as residues of chemicals and PMMA used in wet transfer of graphene, may affect the vdW interface or even block the charge transfer across the R6G/graphene interface. This can lead to a reduced SERS CM enhancement. The UVC irradiation may effectively remove these residues. In addition, the large UVC photon energy may further activate the graphene surface via generation of defects through breaking (at an atomic scale) the C−C bond and formation of C−O groups on graphene. We hypothesize that this UVC-treated graphene has an activated graphene surface for improved R6G probe molecule attachment. In addition, the p-doping on graphene through UVC induced C−O groups and the Pt-NPs decoration on graphene would shift graphene's Fermi energy for an improved charge transfer (CT) effect from R6G molecules.

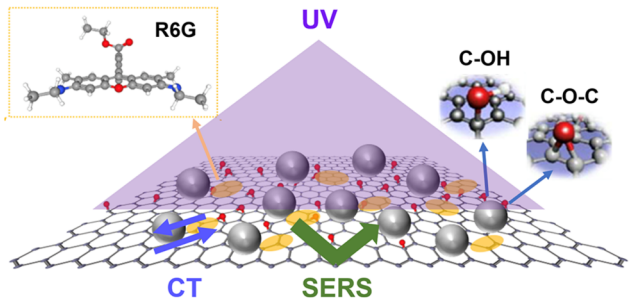

Figure 1. Schematic representation of a graphene SERS substrate with UVC irradiation and Pt-NP (gray spheres) decoration for SERS CM enhancement through improved charge transfer (CT) across the R6G (orange circles)/graphene interface.

2. EXPERIMENTAL METHODS

2.1. Growth of Graphene Using Chemical Vapor Deposition (CVD). Graphene was made on copper sheet that was placed inside quartz tube in the CVD furnace at 1050 °C. The growth time is about 30 min in the flow of a mixed gas of H_2 (7 sccm) and CH_4 (40 sccm), the details of the growth procedure has been described in detail in our earlier works.[36,37] Graphene was then transferred on SiO_2/Si substrates using a wet transfer process.[36,37] Briefly, 3% poly(methyl methacrylate) (PMMA) was spin-coated at 3000 rpm for around 30 s over the graphene/Cu sample, followed with baking at 120 °C for 5 min in air on a hot plate. Afterward, the sample was immersed in the copper etchant (ferric chloride solution $FeCl_3$) for about 3−5 h with the PMMA side facing up until the Cu sheet was completely dissolved. The PMMA/graphene samples were then rinsed with deionized water about five times to detach the chemical residues. The thoroughly cleaned PMMA/graphene samples were then transferred onto the SiO_2 /Si substrates (PMMA side facing up) and left to dry at room temperature overnight to ensure graphene's attachment to the substrate. In order to remove the PMMA, the PMMA/graphene/SiO_2/Si samples were socked in acetone multiple times (~4 times typically) to dissolve PMMA. Rinse with isopropanol (IPA) after each soak was carried out to wash away PMMA residues. Finally, a thermal annealing protocol at 400 °C for 30 min in forming gas of Ar (500 sccm)/H_2 (300 sccm) was applied to the samples to further clean off

https://doi.org/10.1021/acsanm.3c03532
ACS Appl. Nano Mater. 2023, 6, 21626−21633

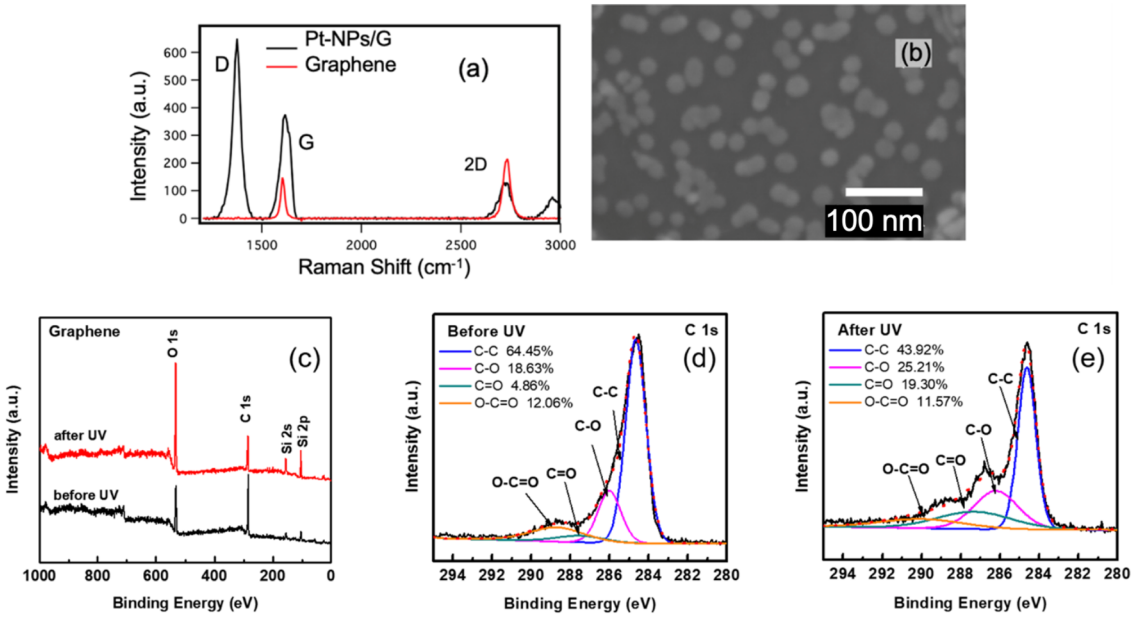

Figure 2. (a) Raman spectra of pristine graphene (red) and Pt-NPs/graphene (G) (in black). (b) SEM image of Pt-NPs on graphene (scale bar: 100 nm). (c) XPS spectra taken on graphene before and after 10 min UVC exposure. (d, e) C 1s peak high-resolution scan. Red dashed lines represent the fitted C 1s peaks and the C 1s peak components that were contributed by different C binding states.

the PMMA residues left on graphene. The thoroughly cleaned graphene surface is critical to sensing.

2.2. Decoration of Pt-NPs on Graphene. The ALD of Pt on graphene was accomplished by using alternating exposures to Trimethyl(methylcyclopentadienyl)-platinum(IV) (MeCpPtMe3, Sigma-Aldrich) and oxygen in a customer-built vacuum reactor at temperature of ~300 °C.[34] During ALD, a constant flow (5 sccm) of ultrahigh-purity nitrogen (99.99%) carrier gas was passed through the reactor. The MeCpPtMe3 precursor was heated to 60 °C to increase the vapor pressure. In each ALD growth cycle consisting of one each of the MeCpPtMe3 and oxygen exposures lasting for ~3 s for MeCpPtMe3 and 1 s for oxygen, respectively, followed with nitrogen purges of 60 s after each exposure to ensure that the precursor reaction only occurs at the sample surface. As shown in our previous studies, Pt-NPs could be conformally coated on carbon nanotubes at low ALD growth cycles below 70.[34,35] Considering the similarity of the surfaces of graphene and carbon nanotubes, 20 cycles were selected in ALD decoration for Pt-NPs on graphene in this work.

2.3. C-Band Ultraviolet (UVC) Irradiation. The UVC irradiation was carried out in an Ozone Cleaner (ProCleaner plus) that has two emission wavelengths of 185 and 254 nm. Specifically, graphene/SiO_2/Si substrates (with or without Pt-NP decoration) were placed in the Ozone Cleaner, and the UVC irradiation was carried out at room temperature of 22 °C for different period in the range of 4−12 min. Since UVC irradiation was found to change the surface of graphene from hydrophobic to hydrophilic, the R6G samples were deposited on the SERS substrates before UVC irradiation to avoid the effect of the graphene surface change on R6G sample deposition. It should be noted that R6G is a dye molecule with an absorption peak located at 532 nm. This means that R6G molecules would absorb UVC photons during UVC irradiation.

2.4. Sample Characterization. Scanning electron microscopy (SEM) image of the graphene decorated with Pt-NPs was taken on Hitachi SU8230 Ultrahigh Resolution Scanning Electron Microscope with a cold cathode field-emission source and e-beam acceleration voltage of 30 keV to extract the information on Pt-NP distribution on graphene surface. X-ray photoelectron spectroscopy (XPS) spectra were obtained at room temperature using a Phi 5000 VersaProbe II X-ray Photoelectron Spectrometer. The spectra were analyzed and processed by using CasaXPS software.

2.5. Raman Spectra of R6G on SERS Substrates. For the investigation of SERS, R6G was used as a probe molecule. A droplet of R6G (diameter around 5 mm) with different concentrations from 5 × 10^{-6} M to 10^{-10} M was placed on the SERS substrate surface and left to dry in air for about 1 h on a hot plate set at 70 °C. The number of R6G molecules on the sample spot was estimated using the R6G concentration in the solution, droplet volume using for making the sample, and the sample size on the SERS substrates For example, at the R6G concentration of 5 × 10^{-6} M, the molecule number in the droplet of 32 mm^3 in volume is about 10^{11} molecules. After the R6G droplet was deposited on the SERS substrate and dried, a sample of a circular spot with an area of approximately 22 mm^2 was formed, which results in the number of molecules per unit area in the spot being ~10^3 molecules/μm^2. SERS spectra were collected using the same WiTec alpha 300 confocal Raman system (laser excitation of 532 nm). The laser beam spot with about tens of mm in diameter that was further reduced through a 20× microscope objective to allow multiple scan spots near the center of the droplet for consistency. An integration time of 3 s and a low excitation intensity ~1−5 mW were used to avoid the possible damage of the R6G probe molecules. For an improved signal-to-noise ratio, each presented Raman spectrum is an average of several spectra gathered at the same spot of the sample. It should be noticed that every Raman spectrum demonstrated in this work are representative based on average of ~10 or more Raman spectra gathered at different spots arbitrarily selected on a sample. Typically 2−3 samples made under the same condition were tested for reproducibility. In order to prevent the coffee-ring effect, the tested spots were chosen not too close to the droplet's edge.

2.6. Graphene Field-Effect Transistor (GFET) Fabrication and Characterization. GFET fabrication started from photolithography to define electrodes on the commercial SiO_2 (90 nm)/Si (doped) substrates, followed by deposition of Nb (40 nm)/Pd (10 nm) via DC sputtering at 75 W/90 W in Ar gas of operating pressure of 14 mTorr/30 mTorr. After electrode liftoff, graphene was wet-transferred on SiO_2 (90 nm)/Si (doped) substrates with the electrodes followed by a second photolithography to define the graphene channels with a channel length of 10 μm and channel width of 20 μm. Reactive ion etching (RIE) of unwanted graphene in oxygen plasma was carried out in a Torr International RIE system. The I_{SD}−V_{BG} curves of the GFET was measured using a probe station connected to an Agilent B1505A semiconductor parameter analyzer.

https://doi.org/10.1021/acsanm.3c03532
ACS Appl. Nano Mater. 2023, 6, 21626−21633

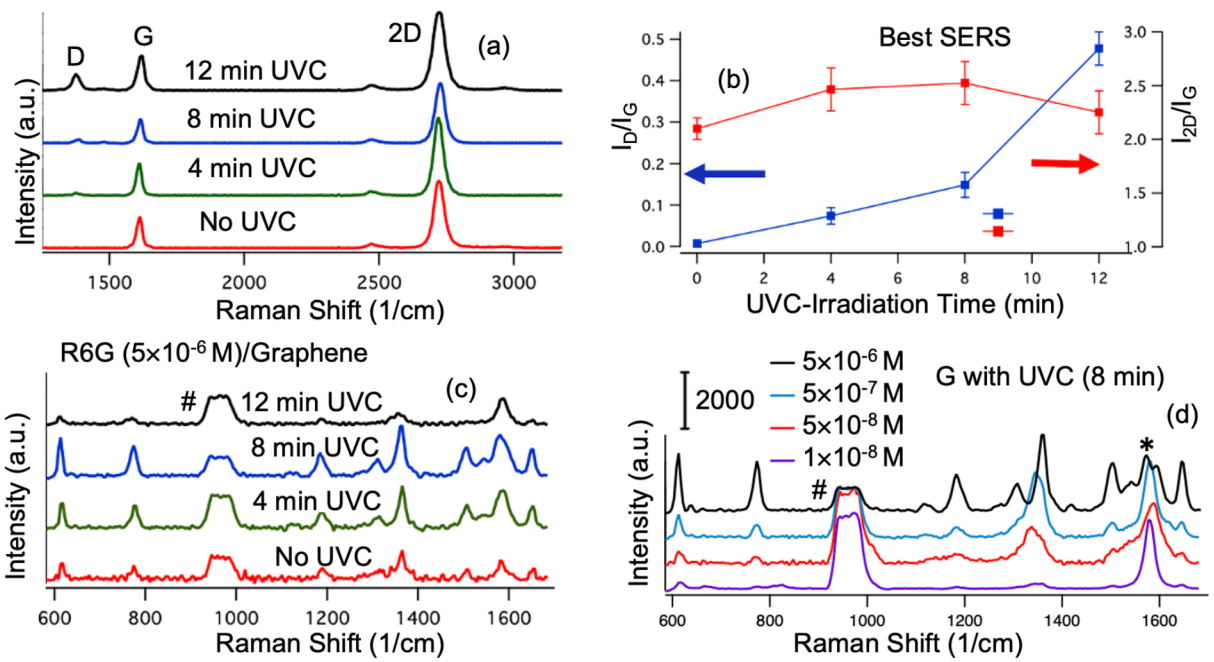

Figure 3. (a) Raman spectra of graphene as a function of UVC-irradiation time including: pristine graphene (red) and graphene after exposing to UVC irradiation for 4 min (green), 8 min (blue), and 12 min (black), respectively. (b) Graphene's Raman peak intensity ratios of I_D/I_G (left-hand side) and I_{2D}/I_G (right-hand side) as a function of the UVC exposure time. (c) Raman spectra of R6G (5×10^{-6} M) taken after different UVC exposure in the range of 4−12 min. (d) Raman spectra of the R6G molecules with different concentrations in the range of 5×10^{-6} M to 1×10^{-8} M on the graphene SERS with UVC exposure of 8 min. The marks # and * donate Si and graphene, respectively.

The light assisted annealing was done by pumping the probe station chamber to 10^{-7} Torr for 48 h, during which a white light illumination was applied on the GFET sample from the viewing port using a flashlight with an intensity of ∼10 mW/cm^2.

3. RESULTS AND DISCUSSION

The Raman spectrum taken on pristine graphene is shown in Figure 2a (in red) with two graphene characteristic peaks: G band is at ∼1580 cm^{-1} and the 2D band at ∼2702 cm^{-1}. The two peaks are associated with the doubly degenerate zone center E_g^2 and the second-order zone-boundary phonon modes, respectively. The intensity ratio of 2D to G band is about 1.8. This together with a negligible D band at ∼1350 cm^{-1} associated with defects suggests that the sample is high-quality single-layer graphene. After Pt-NP decoration, the Raman spectrum was taken again, and the result (black) is compared with the pristine graphene in Figure 2a. Several changes are clearly visible including the reduced ratio of 2D to G peaks to about 0.3 and appearance of the D peak. Both indicate moderate defect formation in graphene, possibly due to the exposure of graphene to oxygen at an elevated temperature of 300 °C for ALD deposition of Pt-NPs. Furthermore, while the G peak has a lightly higher intensity, the 2D peak's intensity is reduced as compared to their pristine graphene counterpart's. This trend differs from the case of Au-NPs/graphene,[10,27] in which both G and 2D peaks show enhanced intensities ascribed to the enhanced EM effect by the localized surface plasmonic resonance (LSPR) effect on Au-NPs. This means that the EM enhancement by Pt-NPs may be considerably smaller than that of Au or Ag-NPs, which may be attributed to the lower conductivity of Pt and hence higher ohmic loss in the LSPR on the surface of the Pt-NPs. This argument is supported by previous reports of low EM enhancement factors in Pt by other groups.[31,33] For example, Tian et al. reported an EM enhancement factor of ∼2000 for roughened Pt,[33] which is significantly lower than that of Au-NPs' up to 10^8−10^{10}. Furthermore, the appearance of the high D peak in graphene after the ALD Pt coating could be attributed to the strong chemical bonding formed between Pt and graphene, which breaks graphene's sp2 crystallinity. This phenomenon was also observed on graphene after coating with various metals including Au[27,38] and Ti.[39] Figure 2b shows an SEM image taken on a representative Pt-NPs/graphene sample. Pt-NPs are clearly visible with a round shape. The lateral dimension of the Pt-NPs is estimated to be 10−20 nm, and the density is around 1000−1500/mm^2. Figure 2c exhibits XPS spectra taken on a UVC-treated graphene before and after 10 min UVC exposure. The peak located at 284.5 eV is corresponding to C 1s on graphene. The other three strong peaks at 532.5 155.1, and 102.9 eV are associated with O 1s, Si 2s, and Si 2p, respectively, which are ascribed to the SiO_2 layer on Si substrates. A high-resolution scan of the C 1s peak specifically was taken, and spectra are shown in Figure 2d,e for graphene before and after UVC exposure, respectively. In order to extract the binding information on C atoms in graphene, C 1s peak fitting using a commercial software CasaXPS was carried out. Results shows that the percentage of C−O and C═O bonds increased after UVC irradiation, indicating graphene was partially oxidized which is probably an effect coming from the Ozone produced during UVC exposure.[40]

Figure 3a compares the Raman spectra of graphene taken after UVC irradiation for different periods of 4−12 min. The Raman spectrum for a pristine graphene (red) is also included, which shows the expected G and 2D peaks with the expected I_{2D}/I_G ∼2.1 and negligible D peak (very small I_D/I_G ∼0.007 for a high-quality, single-layer graphene. After UVC irradiation, the two ratios both exhibit variations with the irradiation time, as shown in Figure 3b. The I_{2D}/I_G ratio (red) has a moderate

https://doi.org/10.1021/acsanm.3c03532
ACS Appl. Nano Mater. 2023, 6, 21626−21633

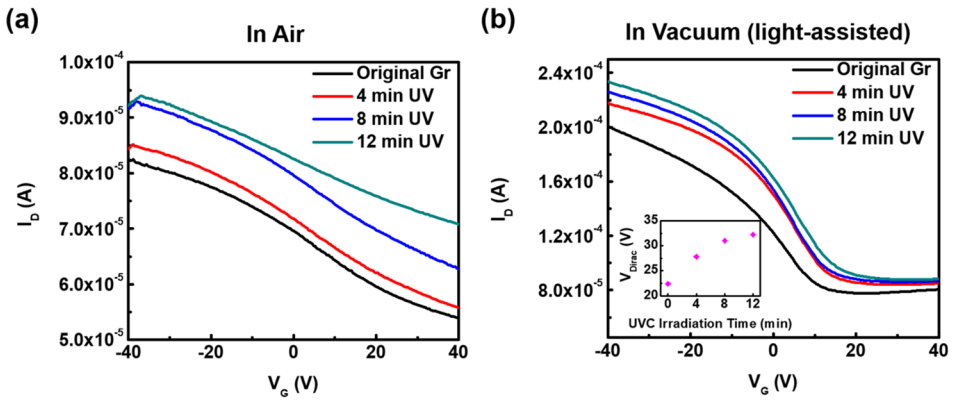

Figure 4. I_D-V_G curves of two GFETs to record position shift after 4, 8, 12, and 16 min UV irradiation. Measured (a) in air (left), and (b) in vacuum with white light (to assist removal of polar molecules adsorbed on graphene, right), respectively. The inset of Figure 4b shows the value of V_{Dirac} as a function of UVC irradiation time.

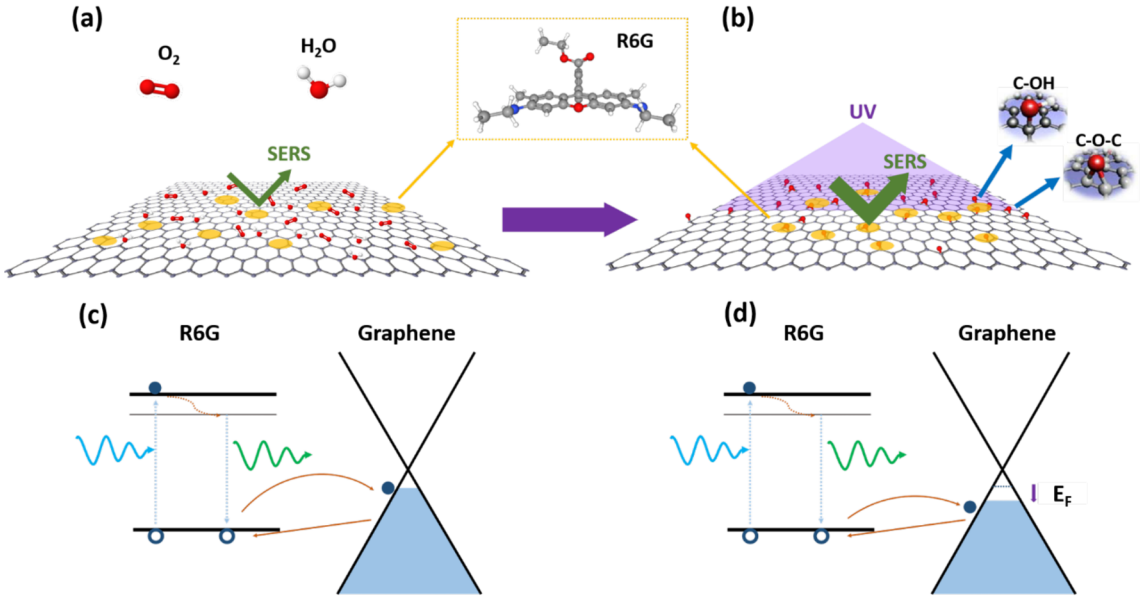

Figure 5. Schematic illustration of SERS on (a) original graphene and (b) UV-treated graphene. C−OH and C−O−C groups formed on graphene after UV irradiation. (c) Charge transfer between R6G and original graphene; (d) Charge transfer between R6G and UV treated graphene. Fermi level of graphene down-shifted after UV irradiation.

variation initially increasing to 2.4 after 4 min UVC exposure, saturated at ∼ 2.5 after 8 min UVC exposure, followed with a decrease to 2.3 after 12 min UVC exposure. Meanwhile, the defect D peak intensity increases with the UVC exposure time. This is shown in the monotonically increasing I_D/I_G ratio (blue) with the UVC exposure time to 0.07 after 4 min UVC exposure, to 0.14 after 8 min UVC exposure, and 0.5 at 12 min UVC exposure. Since D peak intensity reflects the defects in graphene, the monotonically increasing I_D/I_G ratio suggests the UVC irradiation generate defects in graphene, However, since the graphene signature G and 2D peaks, especially their ratio I_{2D}/I_G are more or less not affected by the UV exposure, it seems plausible to assume the UVC irradiation only activate the graphene surface via generation of small-scale or possibly atomic scale activation of the C−C bond on graphene.

Figure 3c compares Raman spectra of R6G (5×10^{-6} M) on pristine graphene (red) and graphene with different UVC exposure times of 4 min (green), 8 min (blue), and 12 min (black). The R6G signature peaks are enhanced on graphene with the two smaller UVC exposure times and the higher enhancement can be seen on the sample with UVC-irradiation for 8 min. Quantitatively, the enhancement factor based on 613 cm^{-1} peak is up to 1.6 after 4 min UVC exposure and increased to 2.7 on the 8 min UVC exposed sample. It should be noted that longer UVC irradiation for 12 min leads to reduced R6G signature peaks and decreased the enhancement factor to 0.7, which indicates the importance to keep the integrity of graphene by balancing the effects of surface activation at smaller scale (positive) and defect formation in larger scale (negative).

Figure 3d compares the Raman spectra of R6G of different concentrations ranging from 5×10^{-6} M to 10^{-8} M. All samples were exposed to UVC for 8 min. Most of the Raman signatures peaks of R6G are visible at R6G concentrations above 5×10^{-8} M. With further reduction of the R6G concentration to 1×10^{-8} M, some Raman signatures peaks, such as at 613 $cm^{-11}$and 1191 cm^{-1}, are still detectable. It should be noted that the R6G sensitivity of 1×10^{-8} M

https://doi.org/10.1021/acsanm.3c03532
ACS Appl. Nano Mater. 2023, 6, 21626−21633

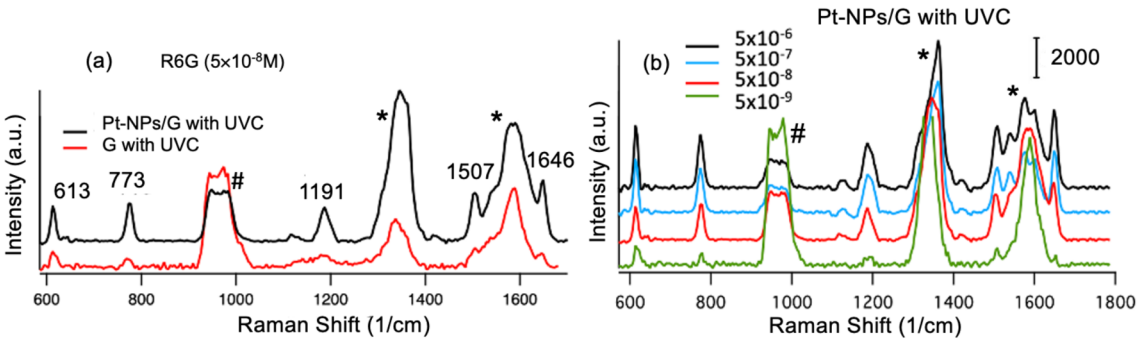

Figure 6. (a) Raman spectra of the R6G molecules of the concentration of 5×10^{-8} M on graphene (G) SERS substrates with 8 min UVC exposure with (black) and without (red) Pt-NPs decoration. (b) Raman spectra of R6G molecules at different concentrations in the range of 5×10^{-6} M to 5×10^{-9}on Pt-NPs/graphene substrate with UVC irradiation for 8 min. The marks of # and * donate Si and graphene, respectively.

achieved here on UVC irradiated graphene is about one and a half orders of magnitude higher than that of 5×10^{-7} M on pristine graphene,[18] indicating a higher CM enhancement on the UVC irradiated graphene.

This enhancement could be due to two effects resulting from UVC irradiation on graphene. The first is the oxidative free radicals (hydroxyl radical HO$^{\bullet}$ or oxygen radical [O]) created under UVC irradiation led to the formation of oxygen groups (e.g., C−OH and C−O−C) on graphene surface,[6,41] which agrees with the XPS result. The oxidized graphene provides higher Raman enhancement than the pristine graphene,[42] as the oxygen-containing functional groups on the graphene were considered for providing favorable sites for better adsorption/attachment of R6G molecules, meanwhile having larger polarizability and strong local dipole moment for the enhanced local electric field enhances the Raman signal.[43,44] The other effect is down-shifting of the graphene Fermi level, i.e. additional p doping in graphene, after UVC irradiation on graphene (Figures 4a and 4b).[6]

The p-doping effect from UVC irradiation was confirmed from recording of I_D-V_G curves of a graphene field effect transistor (GFET) before and after UVC irradiation, measured both in air and in a vacuum with white light assisted (Figure 4). V_{Dirac} was extracted from Figure 4b by taking the differentiation of I_D with respect to V_G, and plotted as a function of UVC irradiation time. An obvious right shift of V_{Dirac} is observed. The enhanced SERS signal from further p-doped graphene could be understood as lowering graphene's Fermi level would facilitate the charge transfer process between the R6G molecule and graphene, thereby enhancing the CM effect, as shown in Figures 5c and 5d.

In order to further improve the CM effect and the sensitivity of graphene SERS substrates, Pt-NPs were decorated on the graphene, followed with UVC exposure of the Pt-NPs/graphene for 8 min. Figure 6a shows Raman spectra of the R6G molecules at a concentration of 5×10^{-8} M on graphene without (red) and with (black) Pt-NPs. Enhanced R6G signature peaks can be clearly seen in the latter as compared to the former, indicating the improvements by UV exposure and Pt-NPs may be combined. Different enhancement factors of ~2.4, 4.8, 2.9, and 3.2 are obtained on Pt-NPs/graphene using Raman peaks at 613, 773, 1191, and 1357 cm^{-1} respectively, and that may be due to more charge transfer between the Pt-NPs and graphene substrate. Furthermore, higher sensitivity of about a half order of magnitude was obtained on the substrate of Pt-NPs/graphene competitor to the one without Pt-NPs. All Raman signatures of R6G are visible at R6G concentration 5×10^{-9} M. With further reduction of the R6G concentration to 1×10^{-9} M, a few R6G vibrational modes, such as 613 and 773 cm^{-1}, with lager polarizability remain visible.

The further enhanced SERS could be explained by the additional p-doping induced by Pt-NPs decoration on UVC irradiated graphene (Figure 7a), which further lowers the

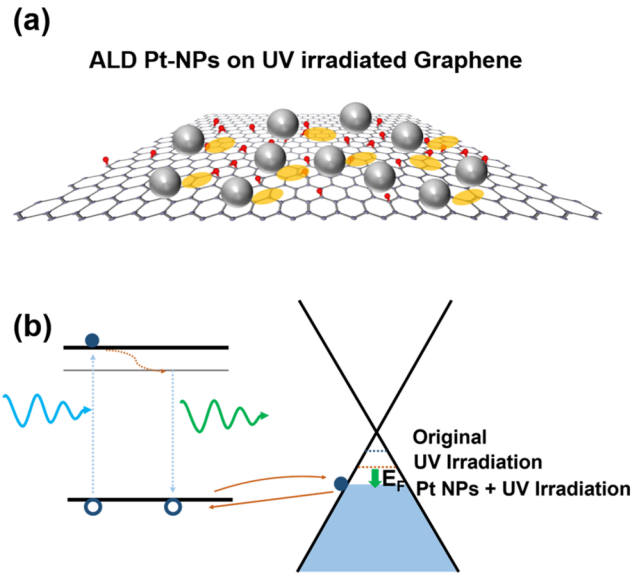

Figure 7. (a) Schematic showing of R6G molecules on Pt-NPs/UV treated graphene platform and (b) CT process between graphene and R6G. Pt NPs push the Fermi level of graphene further downward.

Fermi level of graphene[45] as depicted in Figure 7b, leading to enhanced charge transfer between R6G molecules and graphene. Noted that the Pt-graphene contact as well as UVC irradiation on graphene could both down-shift or p-dope the Fermi level of graphene, which means that these two effects are stackable as shown in our results.

4. CONCLUSION

In summary, a new approach has been developed in this work to enhance the CM effect on graphene SERS substrates. This approach has two components: (1) short-period UVC irradiation of graphene and (2) ALD decoration of Pt-NPs on graphene. The former adopts high-energy C-band UV photons to activate the graphene surface, resulting in a

https://doi.org/10.1021/acsanm.3c03532
ACS Appl. Nano Mater. 2023, 6, 21626−21633

conversion from hydrophobic to hydrophilic surface with oxygen-based functional groups that promote probe molecule attachment and to down-shift the Fermi energy of graphene for enhanced charge transfer from R6G to graphene. The latter further down-shifts the Fermi energy of graphene via hole doping, leading to additional enhancement in charge transfer across the R6G/graphene interface. Using R6G as probe molecules, an enhancement factor of up to 2.7 was obtained on R6G signature peaks in the UVC irradiated graphene SERS substrates with the optimal irradiation time of 8 min. On the Pt-NPs decorated graphene SERS substrates, an additional enhancement factor of 2.5 was obtained on R6G. Interestingly, the two effects can be combined, leading to enhanced R6G SERS sensitivity of 5×10^{-9} M, which is 2 orders of magnitude higher than that on the pristine graphene. This result illustrates a facile approach in engineering the molecule attachment and the energy level alignment at the molecule/graphene interface to enhance the CM effect of graphene as a highly promising SERS substrate for high-sensitivity biosensing.

AUTHOR INFORMATION

Corresponding Authors

Samar Ali Ghopry − *Department of Physics, Jazan University, Jazan 45142, Saudi Arabia; Department of Physics and Astronomy, University of Kansas, Lawrence, Kansas 66045, United States;* orcid.org/0000-0002-2135-8306; Email: sghopry@jazanu.edu.sa

Judy Z. Wu − *Department of Physics and Astronomy, University of Kansas, Lawrence, Kansas 66045, United States*; Email: jwu@ku.edu

Authors

Bo Liu − *Department of Physics and Astronomy, University of Kansas, Lawrence, Kansas 66045, United States;* orcid.org/0000-0003-0298-8238

Andrew Shultz − *Department of Physics and Astronomy, University of Kansas, Lawrence, Kansas 66045, United States;* orcid.org/0009-0007-0106-8903

Complete contact information is available at: https://pubs.acs.org/10.1021/acsanm.3c03532

Author Contributions

S.G. and J.W. proposed the experiment. S.G., B.L., and A.S. provided the characterization of the samples. S.G. and B.L. contributed to sample fabrication. S.G., B.L., and J.W. wrote the manuscript. All authors participated in the improvement of the manuscript.

Notes

The authors declare no competing financial interest.

ACKNOWLEDGMENTS

The authors acknowledge support in part by US National Science Foundation Contracts NSF-DMR-1909292. S.G. acknowledges the support by Jazan University's Deanship of Scientific Research-WAED program W44-87.

REFERENCES

(1) Fang, Y.; Seong, N. H.; Dlott, D. D. Measurement of the distribution of site enhancements in surface-enhanced Raman scattering. *Science* **2008**, *321* (5887), 388−392.

(2) Lin, H. X.; Li, J. M.; Liu, B. J.; Liu, D. Y.; Liu, J.; Terfort, A.; Xie, Z. X.; Tian, Z. Q.; Ren, B. Uniform gold spherical particles for single-particle surface-enhanced Raman spectroscopy. *Phys. Chem. Chem. Phys.* **2013**, *15* (12), 4130−4135.

(3) Potara, M.; Baia, M.; Farcau, C.; Astilean, S. Chitosan-coated anisotropic silver nanoparticles as a SERS substrate for single-molecule detection. *Nanotechnology* **2012**, *23* (5), No. 055501.

(4) Sivashanmugan, K.; Liao, J. D.; Liu, B. H.; Yao, C. K. Focused-ion-beam-fabricated Au nanorods coupled with Ag nanoparticles used as surface-enhanced Raman scattering-active substrate for analyzing trace melamine constituents in solution. *Anal. Chim. Acta* **2013**, *800*, 56−64.

(5) Li, X.; Wu, J.; Mao, N.; Zhang, J.; Lei, Z.; Liu, Z.; Xu, H. A self-powered graphene−MoS2 hybrid phototransistor with fast response rate and high on−off ratio. *Carbon* **2015**, *92*, 126−132.

(6) Huh, S.; Park, J.; Kim, Y. S.; Kim, K. S.; Hong, B. H.; Nam, J. M. UV/ozone-oxidized large-scale graphene platform with large chemical enhancement in surface-enhanced Raman scattering. *ACS Nano* **2011**, *5* (12), 9799−9806.

(7) Guerrini, L.; Graham, D. Molecularly-mediated assemblies of plasmonic nanoparticles for Surface-Enhanced Raman Spectroscopy applications. *Chem. Soc. Rev.* **2012**, *41* (21), 7085−7107.

(8) Mu, C.; Zhang, J. P.; Xu, D. Au nanoparticle arrays with tunable particle gaps by template-assisted electroless deposition for high performance surface-enhanced Raman scattering. *Nanotechnology* **2010**, *21* (1), No. 015604.

(9) Chen, L.; Wu, M.; Xiao, C.; Yu, Y.; Liu, X.; Qiu, G. Urchin-like $LaVO_4$/Au composite microspheres for surface-enhanced Raman scattering detection. *J. Colloid Interface Sci.* **2015**, *443*, 80−87.

(10) Goul, R.; Das, S.; Liu, Q.; Xin, M.; Lu, R.; Hui, R.; Wu, J. Z. Quantitative analysis of surface enhanced Raman spectroscopy of Rhodamine 6G using a composite graphene and plasmonic Au nanoparticle substrate. *Carbon* **2017**, *111*, 386−392.

(11) Zhang, C.; Jiang, S. Z.; Huo, Y. Y.; Liu, A. H.; Xu, S. C.; Liu, X. Y.; Sun, Z. C.; Xu, Y. Y.; Li, Z.; Man, B. Y. SERS detection of R6G based on a novel graphene oxide/silver nanoparticles/silicon pyramid arrays structure. *Opt Express* **2015**, *23* (19), 24811−24821.

(12) Seney, C.; Gutzman, B.; Goddard, R. Correlation of Size and Surface-Enhanced Raman Scattering Activity of Optical and Spectroscopic Properties for Silver Nanoparticles. *J. Phys Chem C* **2009**, *113*, 74.

(13) Stamplecoskie, K. G.; Scaiano, J. C.; Tiwari, V. S.; Anis, H. Optimal Size of Silver Nanoparticles for Surface-Enhanced Raman Spectroscopy. *J. Phys. Chem. C* **2011**, *115* (5), 1403−1409.

(14) Guselnikova, O.; Lim, H.; Kim, H.-J.; Kim, S. H.; Gorbunova, A.; Eguchi, M.; Postnikov, P.; Nakanishi, T.; Asahi, T.; Na, J.; et al. New Trends in Nanoarchitectured SERS Substrates: Nanospaces, 2D Materials, and Organic Heterostructures. *Small* **2022**, *18* (25), 2107182.

(15) Lim, H.; Kim, D.; Kwon, G.; Kim, H.-J.; You, J.; Kim, J.; Eguchi, M.; Nanjundan, A. K.; Na, J.; Yamauchi, Y. Synthesis of Uniformly Sized Mesoporous Silver Films and Their SERS Application. *J. Phys. Chem. C* **2020**, *124* (43), 23730−23737.

(16) Lim, H.; Nagaura, T.; Kim, M.; Kani, K.; Kim, J.; Bando, Y.; Alshehri, S. M.; Ahamad, T.; You, J.; Na, J.; et al. Electrochemical preparation system for unique mesoporous hemisphere gold nanoparticles using block copolymer micelles. *RSC Adv.* **2020**, *10* (14), 8309−8313.

(17) Lim, H.; Kim, D.; Kim, Y.; Nagaura, T.; You, J.; Kim, J.; Kim, H.-J.; Na, J.; Henzie, J.; Yamauchi, Y. A mesopore-stimulated electromagnetic near-field: electrochemical synthesis of mesoporous copper films by micelle self-assembly. *Journal of Materials Chemistry A* **2020**, *8* (40), 21016−21025.

(18) Ghopry, S. A.; Alamri, M. A.; Goul, R.; Sakidja, R.; Wu, J. Z. Extraordinary Sensitivity of Surface-Enhanced Raman Spectroscopy of Molecules on MoS2 (WS2) Nanodomes/Graphene van der Waals Heterostructure Substrates. *Advanced Optical Materials* **2019**, *7* (8), No. 1801249.

(19) Ghopry, S. A.; Sadeghi, S. M.; Berrie, C. L.; Wu, J. Z. MoS2 Nanodonuts for High-Sensitivity Surface-Enhanced Raman Spectroscopy. *Biosensors* **2021**, *11* (12), 477.

(20) Ghopry, S. A.; Sadeghi, S. M.; Farhat, Y.; Berrie, C. L.; Alamri, M.; Wu, J. Z. Intermixed WS2+MoS2 Nanodisks/Graphene van der Waals Heterostructures for Surface-Enhanced Raman Spectroscopy Sensing. *ACS Applied Nano Materials* **2021**, *4* (3), 2941−2951.
(21) Xu, W.; Mao, N.; Zhang, J. Graphene: a platform for surface-enhanced Raman spectroscopy. *Small* **2013**, *9* (8), 1206−1224.
(22) Ling, X.; Xie, L.; Fang, Y.; Xu, H.; Zhang, H.; Kong, J.; Dresselhaus, M. S.; Zhang, J.; Liu, Z. Can Graphene be used as a Substrate for Raman Enhancement? *Nano Lett.* **2010**, *10* (2), 553−561.
(23) Xu, W.; Ling, X.; Xiao, J.; Dresselhaus, M. S.; Kong, J.; Xu, H.; Liu, Z.; Zhang, J. Surface enhanced Raman spectroscopy on a flat graphene surface. *Proc. Natl. Acad. Sci. U. S. A.* **2012**, *109* (24), 9281−9286.
(24) Tan, Y.; Ma, L.; Gao, Z.; Chen, M.; Chen, F. Two-Dimensional Heterostructure as a Platform for Surface-Enhanced Raman Scattering. *Nano Lett.* **2017**, *17* (4), 2621−2626.
(25) Xie, L.; Ling, X.; Fang, Y.; Zhang, J.; Liu, Z. Graphene as a Substrate To Suppress Fluorescence in Resonance Raman Spectroscopy. *J. Am. Chem. Soc.* **2009**, *131* (29), 9890−9891.
(26) Xu, W.; Xiao, J.; Chen, Y.; Chen, Y.; Ling, X.; Zhang, J. Graphene-Veiled Gold Substrate for Surface-Enhanced Raman Spectroscopy. *Adv. Mater.* **2013**, *25* (6), 928−933.
(27) Lu, R.; Konzelmann, A.; Xu, F.; Gong, Y.; Liu, J.; Liu, Q.; Xin, M.; Hui, R.; Wu, J. Z. High sensitivity surface enhanced Raman spectroscopy of R6G on in situ fabricated Au nanoparticle/graphene plasmonic substrates. *Carbon* **2015**, *86*, 78−85.
(28) Ling, X.; Fang, W.; Lee, Y. H.; Araujo, P. T.; Zhang, X.; Rodriguez-Nieva, J. F.; Lin, Y.; Zhang, J.; Kong, J.; Dresselhaus, M. S. Raman enhancement effect on two-dimensional layered materials: graphene, h-BN and MoS2. *Nano Lett.* **2014**, *14* (6), 3033−3040.
(29) Tomašević-Ilić, T.; Jovanović, Đ.; Popov, I.; Fandan, R.; Pedrós, J.; Spasenović, M.; Gajić, R. Reducing sheet resistance of self-assembled transparent graphene films by defect patching and doping with UV/ozone treatment. *Appl. Surf. Sci.* **2018**, *458*, 446−453.
(30) Kim, H.; Lee, D.-H.; Son, Y.-A. Electrochemical Study on Rhodamine 6G-Indole Based Dye for HOMO and LUMO Energy Levels. *Textile Coloration and Finishing* **2013**, *25*, 7.
(31) Yamada, H.; Yamamoto, Y. Surface enhanced Raman scattering (SERS) of chemisorbed species on various kinds of metals and semiconductors. *Surf. Sci.* **1983**, *134* (1), 71−90.
(32) Cai, W. B.; Ren, B.; Li, X. Q.; She, C. X.; Liu, F. M.; Cai, X. W.; Tian, Z. Q. Investigation of surface-enhanced Raman scattering from platinum electrodes using a confocal Raman microscope: dependence of surface roughening pretreatment. *Surf. Sci.* **1998**, *406* (1), 9−22.
(33) Tian, Z.-Q.; Ren, B.; Wu, D.-Y. Surface-Enhanced Raman Scattering: From Noble to Transition Metals and from Rough Surfaces to Ordered Nanostructures. *J. Phys. Chem. B* **2002**, *106* (37), 9463−9483.
(34) Liu, B.; Alamri, M.; Walsh, M.; Doolin, J. L.; Berrie, C. L.; Wu, J. Z. Development of an ALD-Pt@SWCNT/Graphene 3D Nanohybrid Architecture for Hydrogen Sensing. *ACS Appl. Mater. Interfaces* **2020**, *12* (47), 53115−53124.
(35) Alamri, M. A.; Liu, B.; Walsh, M.; Doolin, J. L.; Berrie, C. L.; Wu, J. Z. Enhanced H_2 Sensitivity in Ultraviolet-Activated Pt Nanoparticle/SWCNT/Graphene Nanohybrids. *IEEE Sensors Journal* **2021**, *21* (18), 19762−19770.
(36) Cook, B.; Liu, Q.; Liu, J.; Gong, M.; Ewing, D.; Casper, M.; Stramel, A.; Wu, J. Facile zinc oxide nanowire growth on graphene via a hydrothermal floating method: towards Debye length radius nanowires for ultraviolet photodetection. *Journal of Materials Chemistry C* **2017**, *5* (38), 10087−10093.
(37) Gong, M.; Liu, Q.; Cook, B.; Kattel, B.; Wang, T.; Chan, W.-L.; Ewing, D.; Casper, M.; Stramel, A.; Wu, J. All-Printable ZnO Quantum Dots/Graphene van der Waals Heterostructures for Ultrasensitive Detection of Ultraviolet Light. *ACS Nano* **2017**, *11*, 4114.
(38) Ananthoju, B.; Biroju, R. K.; Theis, W.; Dryfe, R. A. W. Controlled Electrodeposition of Gold on Graphene: Maximization of the Defect-Enhanced Raman Scattering Response. *Small* **2019**, *15* (48), No. 1901555.
(39) Iqbal, M. W.; Singh, A. K.; Iqbal, M. Z.; Eom, J. Raman fingerprint of doping due to metal adsorbates on graphene. *J. Phys.: Condens. Matter* **2012**, *24* (33), No. 335301.
(40) Cheng, Y. C.; Kaloni, T. P.; Zhu, Z. Y.; Schwingenschlögl, U. Oxidation of graphene in ozone under ultraviolet light. *Appl. Phys. Lett.* **2012**, *101* (7), 073110.
(41) Mulyana, Y.; Uenuma, M.; Ishikawa, Y.; Uraoka, Y. Reversible Oxidation of Graphene Through Ultraviolet/Ozone Treatment and Its Nonthermal Reduction through Ultraviolet Irradiation. *J. Phys. Chem. C* **2014**, *118*, 27372.
(42) Yu, X.; Cai, H.; Zhang, W.; Li, X.; Pan, N.; Luo, Y.; Wang, X.; Hou, J. G. Tuning Chemical Enhancement of SERS by Controlling the Chemical Reduction of Graphene Oxide Nanosheets. *ACS Nano* **2011**, *5* (2), 952−958.
(43) Böttcher, C. J. F. Chapter I - Electric Dipoles and Multipoles. *Theory of Electric Polarization*, 2nd ed.; Elsevier, 1973; pp 9−58.
(44) Nir, S.; Adams, S.; Rein, R. Polarizability calculations on water, hydrogen, oxygen, and carbon dioxide. *J. Chem. Phys.* **1973**, *59* (6), 3341−3355.
(45) Chaves, F. A.; Jiménez, D.; Cummings, A.; Roche, S. Physical model of the contact resistivity of metal-graphene junctions. *J. Appl. Phys.* **2014**, *115*, 164513−164513.

https://doi.org/10.1021/acsanm.3c03532
ACS Appl. Nano Mater. 2023, 6, 21626−21633